Magnetic Susceptibility Trends in Oxo-Bridged, Dinuclear Chromium(III) Complexes. Crystal Structure of $[(tmpa)Cr(\mu\text{-}O)(\mu\text{-}CO_3)Cr(tmpa)](ClO_4)_2\cdot 2H_2O$

N. Kent Dalley,[†] Xiaolan Kou,[†] Charles J. O'Connor,[‡] and Robert A. Holwerda*[,§]

Department of Chemistry and Biochemistry, Brigham Young University, Provo, Utah 84602, Department of Chemistry, University of New Orleans, New Orleans, Louisiana 70148, and Department of Chemistry and Biochemistry, Texas Tech University, Lubbock, Texas 79409

Received September 19, 1995[⊗]

The synthesis and physical characterization of oxo-bridged $[Cr_2(tmpa)_2(\mu\text{-}O)(X)]^{n+}$ complexes (tmpa = tris(2-pyridylmethyl)amine) containing a variety of complementary ligands ($X = CO_3^{2-}$, $PhPO_4^{2-}$, HS^-) are described, with the objective of understanding factors underlying variations in the antiferromagnetic coupling constant *J*. We also present the crystal structure of $[(tmpa)Cr(\mu\text{-}O)(\mu\text{-}CO_3)Cr(tmpa)](ClO_4)_2\cdot 2H_2O$, for comparison with previous findings on $[(tmpa)Cr(\mu\text{-}O)(\mu\text{-}CH_3CO_2)Cr(tmpa)](ClO_4)_3$. The carbonate-bridged complex crystallizes in the monoclinic space group $P2_1/c$ with $a = 11.286(10)$ Å, $b = 18.12(2)$ Å, $c = 20.592(12)$ Å, $\beta = 95.99(5)°$, and $V = 4190$ Å^3 and $Z = 4$. Asymmetric tmpa ligation pertains, with apical N atoms situated trans to bridging oxo and acido O atoms. Key structural parameters include $Cr-O_b$ bond lengths of 1.818(6) and 1.838(6) Å, $Cr-OCO_2$ distances of 1.924(7) and 1.934(7) Å, and a bridging bond angle of 128.3(3)°. Several attempts to prepare oxo, amido-bridged dimers were unsuccessful, but the nearlinear $[Cr(tmpa)(N(CN)_2)]_2O(ClO_4)_2\cdot 3H_2O$ complex was isolated from the reaction of dicyanamide ion with $[Cr(tmpa)(OH)]_2^{4+}$. In contrast to the behavior of analogous diiron(III) complexes, antiferromagnetic coupling constants of $[Cr_2(tmpa)_2(\mu\text{-}O)(X)]^{n+}$ dinuclear species are highly responsive to the X group. Considering the complexes with $X = CO_3^{2-}$, $PhPO_4^{2-}$, HS^-, SO_4^{2-}, and RCO_2^- (10 R substituents), we find a reasonably linear, empirical relationship between *J* and oxo bridge basicity, as measured by pK_a (Cr(OH)Cr) values in aqueous solution. While there is no theoretical basis for such a correlation between solid-state and solution-phase properties, this relationship demonstrates that CrOCr π-bonding contributes significantly to antiferromagnetic exchange. Thus, *J* tends to become less negative with increasing $\mu\text{-}O^{2-}$ basicity, showing that greater availability of a bridging oxo group lone pair toward the proton, with decreasing CrOCr π-interaction, reduces the singlet−triplet gap.

Introduction

Oxo-bridged transition metal complexes with complementary bridging ligands are of interest from both bioinorganic[1] and theoretical[2−4] perspectives. While most recent work in this area deals with the bioinorganic chemistry of Fe(III) dinuclear complexes,[5] we have concentrated on Cr(III) dimers, for which relationships among electronic spectra, oxidation potentials and oxo-bridge basicities are particularly informative with regard to electronic structure.[6−15] In this concluding paper of our synthetic series, we describe $[(tmpa)Cr(\mu\text{-}O)(X)Cr(tmpa)]^{n+}$ dinuclear compounds (tmpa = tris(2-pyridylmethyl)amine) with $X = CO_3^{2-}$, $PhPO_4^{2-}$, and HS^-. Structures of hydroxo-bridged[16,17] and unsupported[18] $\mu\text{-}CO_3^{2-}$ Cr(III) dinuclear complexes are known, but the instability of $Cr(\mu\text{-}O)(\mu\text{-}CO_3)Cr$ species with aliphatic amine chelating ligands prevents their characterization in the solid state. We report the structure of $[(tmpa)Cr(\mu\text{-}O)(\mu\text{-}CO_3)Cr(tmpa)](ClO_4)_2\cdot 2H_2O$, for comparison with previous findings on $[(tmpa)Cr(\mu\text{-}O)(\mu\text{-}CH_3CO_2)Cr(tmpa)](ClO_4)_3$[11] and X-ray diffraction results on related Fe(III) species.[19,20]

A correlation between HOMO energy and π-donating ability of bridging and non-bridging ligands has been demonstrated for both singly- and doubly-bridged CrOCr dimers through a linear free energy relationship between $E_{1/2}$(Cr(III,IV/III,III) and pK_a (Cr(μ-OH)Cr).[12,14] Our objective in this paper is to explore the factors underlying variations in the antiferromagnetic coupling constant *J* as a function of the X group in $[(tmpa)Cr(\mu\text{-}O)(X)Cr(tmpa)]^{n+}$ complexes. The Glerup-Hodgson-Pedersen model successfully expresses the singlet-triplet gap ($-2J$) as a function of Cr−O−Cr and dihedral angles in hydroxo-

[†] Brigham Young University.
[‡] University of New Orleans.
[§] Texas Tech University.
[⊗] Abstract published in *Advance ACS Abstracts,* March 15, 1996.

(1) Holm, R. H. *Chem. Rev.* **1987**, *87*, 1401.
(2) Fink, K; Fink, R.; Staemmler, V. *Inorg. Chem.* **1994**, *33*, 6219.
(3) Lin, Z.; Hall, M. B. *Inorg Chem.* **1991**, *30*, 3817.
(4) Dunitz, J. D.; Orgel, L. E. *J. Chem. Soc.* **1953**, 2594.
(5) Kurtz, D. M., Jr. *Chem. Rev.* **1990**, *90*, 585.
(6) Gafford, B. G.; Holwerda, R. A.; Schugar, H. J.; Potenza, J. A. *Inorg. Chem.* **1988**, *27*, 1126.
(7) Gafford, B. G.; Holwerda, R. A. *Inorg. Chem.* **1989**, *28*, 60.
(8) Gafford, B. G.; Holwerda, R. A. *Inorg. Chem.* **1990**, *29*, 4353.
(9) Gafford, B. G.; O'Rear, C.; Zhang, J. H.; O'Connor, C. J.; Holwerda, R. A. *Inorg. Chem.* **1989**, *28*, 1720.
(10) Holwerda, R. A.; Tekut, T. F.; Gafford, B. G.; Zhang, J. H.; O'Connor, C. J. *J. Chem. Soc., Dalton Trans.* **1991**, 1051.
(11) Gafford, B. G.; Marsh, R. E.; Schaefer, W. P.; Zhang, J. H.; O'Connor, C. J.; Holwerda, R. A. *Inorg. Chem.* **1990**, *29*, 4652.
(12) Tekut, T. F.; O'Connor, C. J.; Holwerda, R. A. *Inorg. Chim. Acta* **1993**, *214*, 145.
(13) Holwerda, R. A. *Polyhedron* **1994**, *13*, 737.
(14) Tekut, T. F.; O'Connor, C. J.; Holwerda, R. A. *Inorg. Chem.* **1993**, *32*, 324.
(15) Holwerda, R. A. *Inorg. Chim. Acta,* in press.
(16) Spiccia, L.; Fallon, G. D.; Markiewicz, A.; Murray, K. S.; Riesen, H. *Inorg. Chem.* **1992**, *31*, 1066.
(17) Wieghardt, K.; Schmidt, W.; van Eldik, R.; Nuber, B.; Weiss, J. *Inorg. Chem.* **1980**, *19*, 2922.
(18) Bang, E.; Eriksen, J.; Glerup, J.; Mønsted, L.; Mønsted, O.; Weihe, H. *Acta Chem. Scand.* **1991**, *45*, 367.
(19) Norman, R. E.; Holz, R. C.; Menage, S.; O'Connor, C. J.; Zhang, J. H.; Que, L., Jr. *Inorg. Chem.* **1990**, *29*, 4629.
(20) Norman, R. E.; Yan, S.; Que, L., Jr.; Backes, G.; Ling, J.; Sanders-Loehr, J.; Zhang, J. H.; O'Connor, C. J. *J. Am. Chem. Soc.* **1990**, *112*, 1554.

0020-1669/96/1335-2196$12.00/0 © 1996 American Chemical Society

bridged complexes.[21] Thus, it has been demonstrated that magnetic exchange is highly sensitive to the hybridization state of the bridging oxygen atom. Although an excellent correlation between $-J$ and the shortest Fe−O(bridging) bond length exists for Fe(μ-O)(μ-X)Fe complexes,[22,23] no such relationship pertains in chromium(III) systems.[16] Since bridging oxo group basicity provides a measure of μ-O^{2-} hybridization, we have tested the hypothesis that J should vary systematically with pK_a (Cr(μ-OH)Cr) in dinuclear Cr(III) complexes.

Experimental Section

Materials and Methods. Reagent grade chemicals and distilled solvents were used throughout. $[Cr(tmpa)(OH)]_2(ClO_4)_4\cdot 4H_2O$ and $[(tmpa)Cr(\mu\text{-}O)(\mu\text{-}SO_4)Cr(tmpa)](ClO_4)_2\cdot H_2O$ were taken from laboratory stock.[7,15] Sodium dicyanamide, sodium hydrosulfide monohydrate, sodium thiomethoxide, sodium diethyldithiocarbamate trihydrate, sodium amide, sodium phenoxide, potassium phthalimide, and potassium thioacetate were purchased from Aldrich. Sodium phenylphosphate dihydrate was obtained from Matheson Coleman and Bell. UV−vis and IR (KBr pellet) spectra were acquired on Shimadzu UV-260 and Perkin-Elmer Model 1600 instruments, respectively. Spectrophotometric titrations, cyclic voltammetric scans, and magnetic susceptibility measurements (4−300 K) were carried out and quantitatively interpreted as previously described.[7,9,14] ^{1}H NMR spectra were recorded on a Bruker 200-MHz spectrometer; chemical shifts are reported in parts per million (δ) downfield from TMS. Microanalyses were performed by Desert Analytics; chromium was assayed by the basic peroxide method.[24] ***Caution!*** Perchlorate salts are potentially explosive, particularly at high temperatures, and should be handled in small quantities.

$[Cr(tmpa)(N(CN)_2)]_2O(ClO_4)_2\cdot 3H_2O$. $[Cr(tmpa)(OH)]_2(ClO_4)_4\cdot 4H_2O$ (1.00 g, 0.841 mmol) was refluxed with $NaN(CN)_2$ (1.4975 g, 8.41 mmol) in CH_3CN (100 mL) for 1 h, affording a dark golden-brown solution. The cooled reaction mixture was filtered to remove excess $NaN(CN)_2$ and then evaporated to dryness. This crude material was dissolved in the minimum volume of CH_3CN and reprecipitated from aqueous $LiClO_4$. The purified complex was washed with water and ether prior to air-drying. Yield: 0.64 g, 70%. Anal. Calcd for $[Cr(tmpa)(N(CN)_2)]_2O(ClO_4)_2\cdot 3H_2O$: Cr, 9.6; C, 44.3; H, 3.9. Found: Cr, 9.5; C, 44.3; H, 3.5. IR: 3422 m, 2295 w, 2225 s, 2174 vs, 1609 s, 1483 m, 1438 m, 1364 w, 1289 w, 1121 vs, 1108 vs, 1090 vs, 1032 w, 858 m, 778 m, 626 s cm^{-1}. UV−vis (CH_3CN; λ_{max}, nm (ϵ, M^{-1} cm^{-1})): 303 (7.2×10^3), 351 (1.4×10^4), 414 (2.5×10^3), 450 sh (1.7×10^3). ^{1}H NMR (CD_3CN), δ: 5.02, 5.20, 5.42 (4 py m-H); 5.94, 5.98, 6.12 (8 py m-H); 7.30 (8 py p-H); 7.66 (4 py p-H); 7.79, 7.98, 8.03 (4 py o-H); 8.77, 8.92, 9.22 (8 py *o*-H); broad CH_2 resonance (6−7) not clearly resolved. CV (CH_3CN, 25 °C, 0.1 M N(n-Bu)$_4$ClO$_4$): $E_{1/2} = 1.23 \pm 0.01$ V vs NHE ($\Delta E_p = 0.19$ V). pK_a(Cr(μ-OH)Cr) (25 °C, I = 0.1 M): 2.06 ± 0.05.

$[Cr_2(tmpa)_2(O)(X)](ClO_4)_2\cdot NaClO_4\cdot H_2O$ (X = CO_3^{2-}, $C_6H_5PO_4^{2-}$) and $[Cr_2(tmpa)_2(O)(HS)](ClO_4)_3\cdot 2H_2O$. $[Cr(tmpa)(OH)]_2(ClO_4)_4\cdot 4H_2O$ (1.00 g, 0.841 mmol) was combined with 8.41 mmol of Na_2CO_3 (0.8914 g), $Na_2C_6H_5OPO_3\cdot 2H_2O$ (1.8340 g) or $NaHS\cdot H_2O$ in 50 mL of CH_3CN. The green carbonate and phenylphosphate complexes formed upon refluxing for 1 h, after which excess sodium salts were removed by filtration and supernatants were evaporated to dryness. To neutralize hydroxo-bridged byproducts, one drop of triethylamine was added to crude products redissolved in the minimum volume of CH_3CN. Complexes were then precipitated by the slow addition of ether, filtered, washed with ether, and air-dried. Yield (X = CO_3^{2-}): 0.61 g (66%). Anal. Calcd for $[Cr_2(tmpa)_2(O)(CO_3)](ClO_4)_2\cdot NaClO_4\cdot H_2O$: Cr, 9.5; C, 40.4; H, 3.5. Found: Cr, 9.5; C, 40.7; H, 3.7. IR: 3422 vs, 1609 s, 1510 s, 1440 s, 1350 m, 1286 w, 1088 vs, 1030 w, 942 w, 907 w, 844 w, 769 s, 654 w, 626 s cm^{-1}. After 110 °C drying: Anal. Calcd for $[Cr_2(tmpa)_2(O)(CO_3)](ClO_4)_2\cdot NaClO_4$: C, 41.1; H, 3.4; N, 10.4. Found: C, 41.4; H, 3.2; N, 10.6. Yield (X = $PhPO_4^{2-}$): 0.92 g (90%). Anal. Calcd for $[Cr_2(tmpa)_2(O)(PhPO_4)](ClO_4)_2\cdot NaClO_4\cdot H_2O$: Cr, 8.6; C, 41.6; H, 3.6. Found: Cr, 8.7; C, 41.6; H, 4.0. IR: 3422 s, 1609 s, 1488 m, 1441 m, 1351 w, 1291 w, 1233 w, 1156 w, 1090 vs, 1029 w, 1010 m, 894 m, 767 s, 698 w, 624 s, 560 m cm^{-1}. The HS^- complex was prepared in similar fashion except that the reaction mixture was stirred at ambient temperature for 24 h prior to evaporation of the solvent, during which time the color changed from purple to red-orange and then to olive green. The crude product was redissolved in CH_3CN containing sufficient triethylamine to neutralize hydroxo-bridged impurities, filtered to remove excess sodium hydrosulfide, precipitated with ether, washed with ether, and air-dried. Yield: 0.51 g (57%). Anal. Calcd for $[Cr_2(tmpa)_2(O)(HS)](ClO_4)_3\cdot 2H_2O$: Cr, 9.7; C, 40.5; H, 3.9. Found: Cr, 9.5; C, 40.4; H, 3.7. IR: 3422 s, 1610 s, 1490 m, 1448 m, 1286 w, 1143 vs, 1113 vs, 1088 vs, 1031 m, 944 w, 887 w, 777 m, 627 s cm^{-1}. After drying at 110 °C: Anal. Calcd for $[Cr_2(tmpa)_2(O)(HS)](ClO_4)_3\cdot H_2O$: C, 41.2; H, 3.7; N, 10.7. Found: C, 41.2; H, 3.5; N, 10.6. All three complexes are unstable in aqueous solution; i.e. an attempt to recrystallize the carbonate complex from water afforded $[(tmpa)Cr(\mu\text{-}O)(\mu\text{-}OH)Cr(tmpa)](ClO_4)_3\cdot H_2O$.[7]

$[Cr(tmpa)(OH)]_2(ClO_4)_4\cdot 2H_2NC(O)NH_2$. In an attempt to prepare an oxo-bridged dimer with complementary urea ligands, $[Cr(tmpa)(OH)]_2(ClO_4)_4\cdot 4H_2O$ (1.00 g, 0.841 mmol) was refluxed with urea (1.0103 g, 16.8 mmol) in 100 mL of CH_3CN. A maroon precipitate that formed within 5 min was unchanged after 2 h, when the product was isolated by filtration of the hot reaction mixture. The lavender product was washed with cold CH_3CN and ether prior to air-drying. Yield: 0.77 g (74%). Anal. Calcd for $[Cr(tmpa)(OH)]_2(ClO_4)_4\cdot 2H_2NC(O)NH_2$: Cr, 8.4; C, 36.9; H, 3.8; N, 13.6. Found: Cr, 8.3; C, 36.8; H, 3.7; N, 13.5. IR: 3449 vs, 3363 vs, 1655 s, 1612 s, 1491 w, 1466 w, 1450 m, 1120 vs, 1034 w, 866 m, 662 w, 626 s, 558 m, 514 m cm^{-1}. VIS (CH_3CN): identical to $[Cr(tmpa)(OH)]_2(ClO_4)_4\cdot 4H_2O$.[7]

Reactions of $[Cr(tmpa)(OH)]_2^{4+}$ with Phthalimide, Phosphate, Thiomethoxide, Phenoxide, Amide, Thioacetate, and Diethyldithiocarbamate Anions. Unsuccessful attempts were made to prepare oxo-bridged complexes with complementary bridging ligands through reactions of $[Cr(tmpa)(OH)]_2(ClO_4)_4\cdot 4H_2O$ with 10-fold excesses of phthalimide, phosphate, thiomethoxide, phenoxide, amide, thioacetate, and diethyldithiocarbamate anions in refluxing CH_3CN. Mixtures of dimer cleavage products were isolated in all cases except phthalimide, for which $[Cr_2(tmpa)_2(\mu\text{-}O)(\mu\text{-}OH)](ClO_4)_3\cdot H_2O$[7] was recovered. The blue product recovered from the diethyldithiocarbamate preparation was shown to be $Cr(dtc)_3\cdot H_2O$. Anal. Calcd for $Cr(CS_2N(C_2H_5)_2)_3\cdot H_2O$: C, 35.0; H, 6.3; N, 8.2. Found: C, 35.1; H, 5.8; N, 8.0.

X-ray Diffraction Studies. A single crystal of $[Cr_2(tmpa)_2(\mu\text{-}O)(\mu\text{-}CO_3)](ClO_4)_2\cdot 2H_2O$ was grown by slow diffusion of diethyl ether into a saturated methanolic solution of $[Cr_2(tmpa)_2(\mu\text{-}O)(\mu\text{-}CO_3)](ClO_4)_2\cdot NaClO_4\cdot H_2O$. A suitable dark blue platelet crystal with dimensions $0.12 \times 0.38 \times 0.40$ mm was mounted on a Siemens R3/v automated diffractometer which utilized graphite monochromated Mo Kα radiation ($\lambda = 0.710\,73$ Å). The lattice parameters and orientation matrix were obtained by using a least-squares procedure involving the angles of 50 ($9.96 < 2\theta < 30.03°$) carefully centered reflections. Intensities were measured by using a variable scan speed $2\theta-\theta$ procedure with the scan speed determined by the intensities of individual reflections. Data were collected to a 2θ limit of 40.0° ($(\sin\theta)/\lambda = 0.481$). The index limits were $0 \le h \le 10$, $0 \le k \le 17$, and $-19 \le l \le 19$. A total of 4377 reflections (3932 ($R_{int} = 3.7\%$) independent data) were collected with three standard reflections measured every 97 reflections. There were no systematic changes in the standards which indicated electronic and crystal stability. The space group, $P2_1/c$, was established unambiguously by the systematic absences of the intensity data. Weights based on counting statistics were applied to the data. They were not corrected for absorption or extinction effects.

The crystal structure was solved by using a combination of heavy atom and direct methods. All non-hydrogen atoms in the unit cell were located including two waters of solvation. Positions for the hydrogen atoms bonded to the carbon atoms were calculated based on the known chemical geometry with the C−H bond distance set equal to 0.96 Å. It was possible to find positions for the two hydrogens bonded to OW2

(21) Hodgson, D. In *Magneto-Structural Correlations in Exchange-Coupled Systems*; Willett, R. D., Ed.; Reidel: Dordrecht, The Netherlands, 1985; p 497.
(22) Gorun, S. M.; Lippard, S. J. *Inorg. Chem.* **1991**, *30*, 1625.
(23) Hart, J. R.; Rappe, A. K.; Gorun, S. M. *Inorg. Chem.* **1992**, *31*, 5254.
(24) Deutsch, E. Taube, H. *Inorg. Chem.* **1968**, *7*, 1532.

Table 1. Crystallographic Data for $[(tmpa)Cr(\mu\text{-}O)(\mu\text{-}CO_3)Cr(tmpa)](ClO_4)_2\cdot 2H_2O$[a]

formula: $C_{37}H_{40}Cl_2Cr_2N_8O_{14}$	$Z = 4$
fw = 995.7	temp = 20 °C
space group: $P2_1/c$ (No. 14)	$\mu = 0.724$ mm^{-1}
$a = 11.286(10)$ Å	$\lambda = 0.71073$ Å
$b = 18.13(2)$ Å	no. of reflcns measd: 4377
$c = 20.592(12)$ Å	no. of reflcns with $F > 2.5\sigma(F)$: 2874
$\beta = 95.99(5)°$	$R = 0.0647$
$V = 4190$ Å^3	$R_w = 0.0717$
ρ(calcd) = 1.578 g cm^{-3}	

[a] Uncertainties in the last significant digit are shown in parentheses. $R = \sum||F_o| - |F_c||/\sum|F_o|$. $R_w = [\sum w(|F_o| - |F_c|)^2/\sum(wF_o)^2]^{1/2}$.

in difference maps but only one hydrogen atom bonded to OW1 could be located. All non-hydrogen atoms except the two water oxygen atoms, which had large isotropic thermal parameters, were refined anisotropically. The highly anisotropic thermal parameters of the perchlorate oxygen atoms suggested that these atoms are disordered, but it was not possible to resolve the disorder. The two water oxygen atoms were refined isotropically. All of the hydrogen atoms were allowed to ride on their neighboring heavy atoms during refinement. Isotropic displacement parameters were assigned to the hydrogen atoms and were not refined. Atomic scattering factors were obtained from ref 31. All programs used in the solution, refinement and display of the title compound are included in the SHELXTL-PLUS (VMS) program package. Crystallographic data and refinement details are given in Table 1. Table 2 presents final atom coordinates and isotropic displacement parameters.

Results and Discussion

Preparations of Dinuclear Chromium(III) Compounds. Dinuclear complexes of the type $[(tmpa)Cr(\mu\text{-}O)(X)Cr(tmpa)]^{n+}$ ($X = CO_3^{2-}$, $PhPO_4^{2-}$ and HS^-) were prepared in good yields through the displacement of H_2O from $[Cr(tmpa)(OH)]_2^{4+}$ by the incoming anion. The carbonate and phenylphosphate complexes co-crystallize with $NaClO_4$ when isolated from acetonitrile solution. Heating displaced the water molecule of crystallization from $[Cr_2(tmpa)_2(\mu\text{-}O)(\mu\text{-}CO_3)](ClO_4)_2\cdot NaClO_4\cdot H_2O$, but only one of two H_2O molecules in the HS^- complex could be removed in this way. The μ-HS^- linkage is well-documented,[25] but we cannot differentiate between $[Cr(\mu\text{-}O)(\mu\text{-}HS)Cr]$ and $[(H_2O)Cr(\mu\text{-}O)Cr(HS)]$ structural formulations of $[Cr_2(tmpa)_2(\mu\text{-}O)(HS)](ClO_4)_3\cdot 2H_2O$ on the basis of solution-phase physical properties. Although phenylphosphate evidently functions as a bridging ligand in $[Fe_2(tmpa)_2(O)(PhPO_4)](ClO_4)_2$,[19,20] the characterization of $[Cr_2(tmpa)_2(O)(PhPO_4)](ClO_4)_2\cdot NaClO_4\cdot H_2O$ presented here permits no distinction between bridging and nonbridging $PhPO_4^{2-}$ roles; the presence of a strongly bent CrOCr unit is clearly apparent, however.

Electronic spectra, oxo-bridge basicities, antiferromagnetic coupling constants and half-wave, one-electron oxidation potentials are presented in Table 3. Nearultraviolet spectra resemble those of $[Cr_2(tmpa)_2(\mu\text{-}RCO_2)(\mu\text{-}O)]^{3+}$ complexes,[11,12] for which the strong, $e_g \rightarrow e_u^*$ charge-transfer band near 28 600 cm^{-1} in linear CrOCr species splits into two components of lesser intensity, at lower ($b_2 \rightarrow a_1$; ca. 27 000 cm^{-1}) and higher ($a_2 \rightarrow b_1$; ca. 30 000 cm^{-1}) energies, under the influence of CrOCr bending (pseudo-C_{2v} symmetry). The weaker $b_1 \rightarrow a_1$ feature near 23 000 cm^{-1} for all three new complexes is red-shifted by ca. 700 cm^{-1} relative to the μ-RCO_2^- complexes. Half-wave oxidation potentials calculated for CO_3^{2-} (0.80 V), $PhPO_4^{2-}$ (0.91 V), and HS^- (0.77 V) complexes on the basis of the linear free energy relationship:[14] $E_{1/2} = 1.40 - 0.10(pK_a)$ V are in good agreement with experimental findings. A similar relationship between one-electron reduction potentials and bridging ligand basicity has been established for $[(tmpa)Fe(\mu\text{-}O)(\mu\text{-}X)Fe(tmpa)]^{n+}$ species; i.e. $E_{1/2}$(Fe(III,III/III,II) becomes more negative with increasing transfer of electron density from

Table 2. Positional Parameters ($\times 10^4$) and Equivalent Isotropic Displacement Coefficients (Å^2 $\times$ 10^3) for Non-Hydrogen Atoms of $[(tmpa)Cr(\mu\text{-}O)(\mu\text{-}CO_3)Cr(tmpa)](ClO_4)_2\cdot 2H_2O$[a]

	x	*y*	*z*	*U*(eq)
Cr1	82(1)	1978(1)	3441(1)	38(1)
Cr2	−2543(1)	1996(1)	2580(1)	47(10)
N1	336(6)	1283(4)	4252(3)	41(3)
C2	−464(9)	1572(6)	4718(5)	58(4)
C3	−391(7)	2394(6)	4750(5)	49(4)
N4	−180(6)	2713(5)	4175(4)	42(3)
C5	−155(8)	3438(7)	4143(5)	55(4)
C6	−353(10)	3888(6)	4661(7)	68(5)
C7	−581(10)	3562(8)	5228(7)	80(6)
C8	−585(9)	2821(7)	5288(5)	66(5)
C9	1612(8)	1268(6)	4539(5)	64(4)
C10	2391(9)	1808(5)	4257(5)	45(4)
N11	1917(6)	2157(4)	3719(4)	43(3)
C12	2618(9)	2628(5)	3419(5)	54(4)
C13	3769(1)	2773(6)	3661(6)	64(5)
C14	4220(10)	2407(6)	4219(6)	65(5)
C15	3542(9)	1920(6)	4516(5)	59(4)
C16	−52(9)	546(5)	3992(5)	58(4)
C17	385(8)	414(6)	3347(5)	45(4)
N18	497(6)	1018(4)	2987(4)	40(3)
C19	824(7)	939(6)	2376(6)	51(4)
C20	1057(8)	248(7)	2116(5)	58(4)
C21	939(9)	−353(7)	2502(7)	68(5)
C22	596(9)	−279(6)	3106(6)	65(5)
O23	181(5)	2677(3)	2746(3)	52(2)
C24	−368(9)	2716(5)	2162(5)	44(4)
O25	−1394(6)	2414(4)	2049(3)	75(3)
O26	79(6)	3034(3)	1711(3)	61(3)
O27	−1513(5)	1758(3)	3287(3)	40(2)
N28	−3854(7)	2257(5)	1787(4)	66(4)
C29	−3472(10)	1842(8)	1210(4)	87(6)
C30	−3080(10)	1094(9)	1400(7)	77(6)
N31	−2534(7)	1040(6)	2014(4)	61(4)
C32	−2162(9)	388(8)	2240(6)	75(5)
C33	−2278(12)	−235(8)	1839(8)	100(7)
C34	−2805(14)	−170(11)	1213(9)	118(9)
C35	−3215(12)	483(10)	985(7)	97(7)
C36	−3796(10)	3053(8)	1729(7)	95(6)
C37	−3719(10)	3405(8)	2400(7)	70(6)
N38	−3101(6)	2998(5)	2876(5)	57(3)
C39	−2985(8)	3252(6)	3496(7)	63(5)
C40	−3425(10)	3930(7)	3665(7)	80(5)
C41	−4071(12)	4323(7)	3154(10)	98(7)
C42	−4223(12)	4045(9)	2543(9)	99(7)
C43	−5064(8)	2044(6)	1947(5)	65(4)
C44	−5030(9)	1557(5)	2529(5)	44(4)
N45	−4022(6)	1522(4)	2935(4)	40(3)
C46	−3981(8)	1105(5)	3476(5)	47(4)
C47	−4954(9)	714(5)	3633(5)	49(4)
C48	−5992(9)	744(6)	3225(6)	58(5)
C49	−6031(8)	1159(6)	2668(5)	56(4)
Cl1	3225(3)	−827(2)	4671(1)	61(1)
O1	3148(8)	−1562(4)	4850(5)	123(5)
O2	2834(7)	−370(4)	5166(3)	89(3)
O3	2597(10)	−682(6)	4083(4)	170(6)
O4	4450(9)	−737(5)	4609(5)	136(5)
Cl2	2800(3)	4020(2)	5540(2)	79(1)
O5	2583(12)	3523(6)	5060(6)	178(7)
O6	2093(8)	4638(5)	5392(5)	121(4)
O7	3933(9)	4182(7)	5634(9)	249(10)
O8	2429(11)	3665(7)	6101(5)	174(6)
OW1	2270(15)	2931(9)	1417(9)	281(8)
OW2	2816(20)	4232(9)	1402(8)	342(11)

[a] Equivalent isotropic *U* defined as one-third of the trace of the orthogonalized $\mathbf{U}_{ij}$ tensor. Uncertainties are shown in parentheses.

(25) Shih, K.-Y.; Fanwick, P. E.; Walton, R. A. *Inorg. Chem.* **1992**, *31*, 3663.

Table 3. Physical Properties of $[(tmpa)Cr(\mu\text{-}O)(X)Cr(tmpa)]^{(4-n)+}$ Complexes

X^{n-}	λ_{max}, nm (ϵ, $mM^{-1}\ cm^{-1}$)[a]	pK_a[b]	J, cm^{-1} [c]	$E_{1/2}$, V vs NHE[d]	ref
OH^-	370 (0.90)	7.50	−68.5	0.62	7, 8, 9
F^-	298 (4.7)	6.25		0.74	8, 14
	330 (4.6)				
	386 (2.9)				
	418 (2.5)				
HS^-	290 sh (5.4)	6.30 (0.05)	−36.2	0.82	this work
	336 (3.9)				
	372 (3.1)				
	430 (1.9)				
CO_3^{2-}	291 sh (5.0)	6.02 (0.04)	−30.4	0.81	this work
	330 pl (3.7)				
	374 (2.8)				
	432 (2.1)				
$C_6H_5OPO_3^{2-}$	291 pl (4.8)	4.94 (0.10)	−42.4	0.91	this work
	337 (4.1)				
	372 (3.3)				
	434 (2.3)				
SO_4^{2-}	304 (5.1)	3.6[e]	−64.0	1.04	this work,
	349 (6.8)				15
	361 sh (6.1)				
	388 (2.6)				
	420 (2.4)				
	457 sh (1.8)				
HCO_2^-	336 (5.5)	1.69	−93.0	1.21	11
	372 (3.6)				
	388 sh (2.2)				
	419 (2.1)				
$CH_3CO_2^-$	336 (4.1)	2.20	−50.3	1.17	11
	372 (2.9)				
	388 sh (2.1)				
	419 (1.8)				
$C_6H_5CO_2^-$	337 (5.4)	1.88	−75.4	1.22	11
	371 (3.5)				
	388 sh (2.5)				
	419 (2.3)				

[a] In CH_3CN solution. [b] pK_a based on the ionization constant of conjugate Cr(OH)Cr acid, at 25.0 °C and $I = 0.1$ M ($NaNO_3$). Standard deviations are shown in parentheses. [c] Antiferromagnetic coupling cosntant. [d] Cr(III,IV/III,III) half-wave reduction potential, measured at 25.0 °C, $I = 0.1$ M (TBAP) in CH_3CN, and 50 mV/s sweep rate. Uncertainty was estimated at ±0.01 V. [e] pK_a estimated from $E_{1/2}$ on the basis of correlation from ref 14.

basic bridging ligands to the diiron core.[26] Consistent with the observation that $[(tmpa)Fe(\mu\text{-}O)(\mu\text{-}CO_3)Fe(tmpa)]^{2+}$ is most difficult to reduce because of high carbonate basicity,[26] we find that $[(tmpa)Cr(\mu\text{-}O)(\mu\text{-}CO_3)Cr(tmpa)]^{2+}$ ranks among the most easily oxidized, doubly-bridged Cr(III) analogs.

Dinuclear products with both O- and N-donor bridging ligands could not be prepared through reactions of the diol precursor with amido or imido anions; $NaNH_2$ and potassium phthalimide afforded dimer cleavage products and $[(tmpa)Cr(O)(OH)Cr(tmpa)](ClO_4)_3\cdot H_2O$,[7] respectively. In the the case of $N(CN)_2^-$, a pseudohalide ligand,[27] the product was $[Cr(tmpa)(N(CN)_2)]_2O(ClO_4)_2\cdot 3H_2O$, an unsupported CrOCr complex whose spectroscopic, electrochemical, and acid−base properties strongly resemble those of related species.[9,14] Thus, $[Cr(tmpa)(N(CN)_2)]_2O^{2+}$ exhibits an asymmetric CrOCr stretching mode at 858 cm^{-1}, intense $e_g \rightarrow e_u^*$ (28 500 cm^{-1}) and $b_{2g} \rightarrow e_u^*$ (24 200 cm^{-1}) electronic transitions, and $E_{1/2}$(Cr(III,IV/III,III) and pK_a(Cr(OH)Cr) values similar to those of $[Cr(tmpa)(NCS)]_2O^{2+}$ ($E_{1/2} = 1.17$ V; $pK_a = 2.05$).[9] We note, however, that the dicyanamide complex exhibits splittings of pyridyl *o*- and *m*-H NMR resonances that were not observed for any of the other pseudohalide complexes,[14] although ratios of integrated peak intensities are still consistent with a geometry in which both apical tmpa N atoms are trans to $N(CN)_2^-$ ligands. Such splitting is anticipated for the nonlinear $N(CN)_2^-$ ligand, provided that rotation about the $Cr-N(CN)_2$ bond is slow on the NMR time scale.

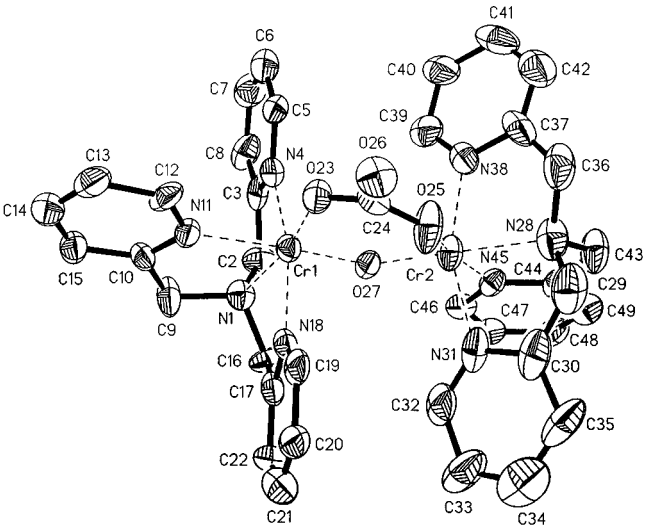

Figure 1. Structure of the $[(tmpa)Cr(\mu\text{-}O)(\mu\text{-}CO_3)Cr(tmpa)]^{2+}$ cation shown with 50% probability ellipsoids. Hydrogen atoms have been omitted for clarity.

It has not been possible to prepare either $[Cr(tmpa)X]_2O^{4+}$ or $[(tmpa)Cr(\mu\text{-}O)(\mu\text{-}X)Cr(tmpa)]^{4+}$ complexes with neutral X groups, presumably because it is difficult to displace an H_2O leaving group when the incoming ligand does not reduce the effective charge at the Cr(III) centers. An attempt to prepare a urea adduct afforded a new complex, however, with the formula $[Cr(tmpa)(OH)]_2(ClO_4)_4\cdot 2H_2NC(O)NH_2$. We conclude that urea functions solely as a molecule of crystallization, probably by hydrogen-bonding to the μ-OH^- ligands, since the C=O stretching mode decreases from 1683 (free urea) to 1655 cm^{-1} in a complex whose visible spectrum is identical to that of the diol precursor.

Structure of $[(tmpa)Cr(\mu\text{-}O)(\mu\text{-}CO_3)Cr(tmpa)](ClO_4)_2\cdot 2H_2O$. The crystal structure of $[(tmpa)Cr(\mu\text{-}O)(\mu\text{-}CO_3)Cr(tmpa)](ClO_4)_2\cdot 2H_2O$ confirmed the presence of bridging oxo and carbonato groups, accompanied by distorted octahedral CrN_4O_2 coordination spheres about both Cr(III) centers. Principal bond lengths and angles within the $[(tmpa)Cr(\mu\text{-}O)(\mu\text{-}CO_3)Cr(tmpa)]^{2+}$ cation (Figure 1) are shown in Table 4. A comparison of bonding parameters for $[(tmpa)Cr(\mu\text{-}O)(\mu\text{-}CO_3)Cr(tmpa)]^{2+}$ and $[(tmpa)Cr(\mu\text{-}O)(\mu\text{-}CH_3CO^2)Cr(tmpa)]^{3+}$ is presented in Table 5. Both exhibit asymmetric tmpa coordination, in which one apical N atom (N28) is trans to the oxo bridge (O27) while the other (N1) is trans to an acido O atom (O23). Average $Cr-O_b$ and Cr−N(pyridyl) bond distances are essentially identical in the μ-CO_3^{2-} and μ-$CH_3CO_2^-$ dinuclear complexes, while Cr−N(tertiary) bonds are slightly longer in the carbonate complex. The OW1−O26 distance (2.616(3) Å) is less than the sum of van der Waals radii for the two oxygen atoms (2.8 Å), consistent with the presence of a water-bridging carbonate hydrogen bond. The crystal structure of $[(tren)Cr(\mu\text{-}OH)(\mu\text{-}CO_3)Cr(tren)](ClO_4)_3\cdot 2H_2O$ not only revealed a much longer $Cr-O_b$ distance (1.944 Å), but both apical N atoms of the tripodal tren ligand are trans to the hydroxo bridge.[16]

(26) Holz, R. C.; Elgren, T. E.; Pearce, L. L.; Zhang, J. H.; O'Connor, C. J.; Que, L., Jr. *Inorg. Chem.* **1993**, *32*, 5844.
(27) *Chemistry of the Pseudohalides*; Golub, A. M.; Kohler, H.; Skopenko, V. V., Eds.; Elsevier: New York, 1986.

Table 4. Principal Distances (Å) and Angles (deg) in $[(tmpa)Cr(\mu\text{-}O)(\mu\text{-}CO_3)Cr(tmpa)](ClO_4)_2\cdot 2H_2O$[a]

Cr1−O23	1.924(7)	Cr2−O25	1.934(7)
Cr1−O27	1.838(6)	Cr2−O27	1.818(6)
Cr1−N1	2.089(7)	Cr2−N28	2.140(8)
Cr1−N4	2.060(9)	Cr2−N31	2.090(10)
Cr1−N11	2.116(7)	Cr2−N38	2.038(9)
Cr1−N18	2.053(8)	Cr2−N45	2.078(8)
N1−Cr1−N4	79.8(3)	O25−Cr2−O27	97.8(3)
N1−Cr1−N11	80.0(3)	O25−Cr2−N28	86.2(3)
N4−Cr1−N11	85.0(3)	O27−Cr2−N28	176.0(3)
N1−Cr1−N18	80.4(3)	O25−Cr2−N31	88.1(3)
N4−Cr1−N18	160.0(3)	O27−Cr2−N31	102.2(3)
N11−Cr1−N18	89.4(3)	N28−Cr2−N31	78.5(4)
O23−Cr1−N1	168.2(3)	N38−Cr2−O25	93.8(3)
N4−Cr1−O23	98.2(3)	O27−Cr2−N38	99.4(3)
N11−Cr1−O23	88.2(3)	N28−Cr2−N38	79.7(4)
N18−Cr1−O23	100.7(3)	N31−Cr2−N38	157.9(3)
O27−Cr1−N1	93.3(3)	N45−Cr2−O25	166.2(3)
N4−Cr1−O27	93.1(3)	O27−Cr2−N45	95.2(3)
N11−Cr1−O27	173.3(3)	N28−Cr2−N45	81.0(3)
N18−Cr1−O27	90.2(3)	N31−Cr2−N45	84.5(3)
O23−Cr1−O27	98.4(3)	N38−Cr2−N45	88.8(3)

[a] Uncertainties in the last significant digit are shown in parentheses.

Table 5. Comparison of Bonding Parameters in $[(tmpa)Cr(\mu\text{-}O)(\mu\text{-}X)Cr(tmpa)]^{n+}$ Dinuclear Complexes with Carbonate and Acetate Complementary Bridging Ligands[a]

parameter	$[Cr_2(tmpa)_2(O)(CO_3)]^{2+}$	$[Cr_2(tmpa)_2(O)(CH_3CO_2)]^{3+}$
$Cr-O_b$, Å	1.818(6), 1.838(6)	1.789, 1.853
Cr−O−Cr, deg	128.3(3)	131.9
Cr−Cr, Å	3.289(4)	3.326
Cr−N(tertiary), Å	2.089(7), 2.140(8)	2.050, 2.115
av Cr−N(pyridyl), Å	2.072	2.062
Cr−O(acido), Å	1.924(7), 1.934(7)	1.931, 1.970
oxo trans influence,[b] Å	0.038	0.055
O−C−O,[c] deg	118.9(9)	127.1
C−O, Å	1.280(12), 1.295(12), 1.246(13)[d]	1.264, 1.265

[a] Data for the oxo, acetato-bridged complex from ref 11. [b] Defined as the difference between Cr−N(pyridyl) bond lengths trans to oxo O and acido O atoms. [c] Corresponds to the bridging O−C−O unit. [d] Corresponds to the C−O bond to the noncoordinated oxygen atom.

The Cr−O(acido) bond length is only nominally shorter in the carbonate-bridged dimer, in contrast to the much larger variance (0.07 Å) between Fe−OCO_2 and Fe-$OC(O)CH_3$ distances in the Fe(III) analogs.[19,20] As compared with the Fe−O−Fe bond angles of $[(tmpa)Fe(\mu\text{-}O)(\mu\text{-}CO_3)Fe(tmpa)]^{2+}$ (125.4°) and $[(tmpa)Fe(\mu\text{-}O)(\mu\text{-}CH_3CO_2)Fe(tmpa)]^{3+}$ (129.7°), Cr−O−Cr angles are consistently larger but the carbonate complex is more strongly bent by ca. 4° in both systems. As a consequence, nonbonding Cr−Cr separations are approximately 0.1 Å larger relative to the Fe−Fe distances. The most significant contrast between high-spin, d^5 Fe(III) and d^3 Cr(III) dinuclear complex series is an enhancement of average Fe−N(pyridyl) (2.15 Å) and Fe−N(tertiary) (2.22 Å) bond lengths, associated with the presence of e_g electrons in the Fe(III) complexes.

Least squares planes were calculated for the three pyridine groups of each tmpa ligand and also for a plane consisting of O23, O25, O26, and O27, the three carbonate oxygen atoms and the bridging oxygen atom. The average deviation of an atom from its least-squares plane for the aromatic groups ranged from 0.001 to 0.014 Å. The dihedral angles between these planes gave no indication of stacking interactions between pyridines on opposite sides of the bridging groups. The dihedral angle between the plane consisting of C10−C15 and the one defined by C30−C35 was 37.5° while the related angle between the C17−C22 and C37−C42 planes was 39.4°. It is interesting to note that the average deviation of an oxygen atom from the O23, O25, O26, O27 plane was only 0.049 Å; Cr1 and Cr2 are 0.476 Å below and 0.392 Å above this oxygen plane, respectively.

Correlation of Antiferromagnetic Coupling Constants with Oxo Bridge Basicity. Magnetic susceptibility measurements showed antiferromagnetic coupling between the Cr(III) centers of oxo-bridged complexes reported here, consistent with the Heisenberg exchange Hamiltonian: $H = -2JS_1\cdot S_2$. Coupling constants are given in Table 3 for $Cr(\mu\text{-}O)(X)Cr$ species with $X = CO_3^{2-}$, $PhPO_4^{2-}$, HS^-, and SO_4^{2-} and are compared with previous findings for $X = \mu\text{-}OH^-$ and $\mu\text{-}RCO_2^-$. The $[Fe_2(tmpa)_2(\mu\text{-}O)(\mu\text{-}X)]^{n+}$ dimers with $X = CO_3^{2-}$ ($J = -108.4$ cm^{-1}),[19] $PhPO_4^{2-}$ ($J = -110.6$ cm^{-1}),[20] SO_4^{2-} ($J = -106.6$ cm^{-1}),[26] and $CH_3CO_2^-$ ($J = -114.3$ cm^{-1})[20] have uniformly larger coupling constants which are insensitive to variations in both the X group and the Fe−O−Fe bond angle.[19,20,26] In contrast, magnetic coupling strength in $Cr(\mu\text{-}O)(X)Cr$ complexes is highly responsive to substituent variations. The nearultraviolet spectra of FeOFe dimers, dominated by oxo-to-Fe(III) LMCT transitions,[28] appear to be more substituent-dependent[19,20,26] with regard to both transition energy and intensity as compared with Cr(III) complexes in the family $[(tmpa)Cr(\mu\text{-}O)(X)Cr(tmpa)]^{n+}$, for which the dominant features have MLCT character.[9]

Antiferromagnetic coupling strength in CrOCr dimers is a function of bridging oxygen atom hybridization, electronic and steric influences on the CrOCr bond angle, the $Cr-O_b$ bond length and nonbonding Cr···Cr separation, crystal packing effects and magnetic exchange mediated by hydrogen bonding.[16,21,29,30] In terms of a molecular orbital description,[4,11] the $b_1(HOMO)-a_2(LUMO)$ energy difference could also contribute to the observed singlet−triplet gap.[14] Considering the dinuclear complexes with $X = CO_3^{2-}$, $PhPO_4^{2-}$, HS^-, SO_4^{2-}, and RCO_2^- with 10 different R groups, we find a reasonably good empirical relationship between J and oxo bridge basicity, as measured by pK_a(Cr(OH)Cr) values in aqueous solution (Figure 2). While there is no theoretical basis for such a correlation between solid-state and solution-phase properties, this relationship demonstrates that CrOCr π-bonding contributes significantly to antiferromagnetic exchange. Thus, J tends to become less negative with increasing $\mu\text{-}O^{2-}$ basicity, showing that greater availability of a bridging oxo group lone pair toward the proton, with decreasing CrOCr π-interaction, reduces the singlet−triplet gap. For reasons that are not clear, the point for $X = OH^-$ (not shown) falls well below the least squares line defined by the other X substituents.

Interpretation of our magnetic findings in light of recent theoretical developments on the superexchange mechanism[2] is instructive. It has been noted that magnetic exchange in Cr(III) dimers cannot be understood solely on the basis of a molecular orbital treatment, which does not correctly take into account the balance between covalent and ionic terms of the wavefunctions for the different spin states which arise from the coupling of $S = {}^3/_2$ metal centers. On the basis of first and

(28) Brown, C. A.; Remar, G. J.; Musselman, R. L.; Solomon, E. I. *Inorg. Chem.* **1995**, *34*, 688.
(29) Glerup, J.; Hodgson, D. J.; Pedersen, E. *Acta Chem. Scand.* **1983**, *A37*, 161.
(30) Goodson, P. A.; Glerup, J.; Hodgson, D. J.; Michelsen, K.; Rychlewska, U. *Inorg. Chem.* **1994**, *33*, 359.
(31) *International Tables for X-ray Crystallography*; Kynch Press: Birmingham, England, 1974.

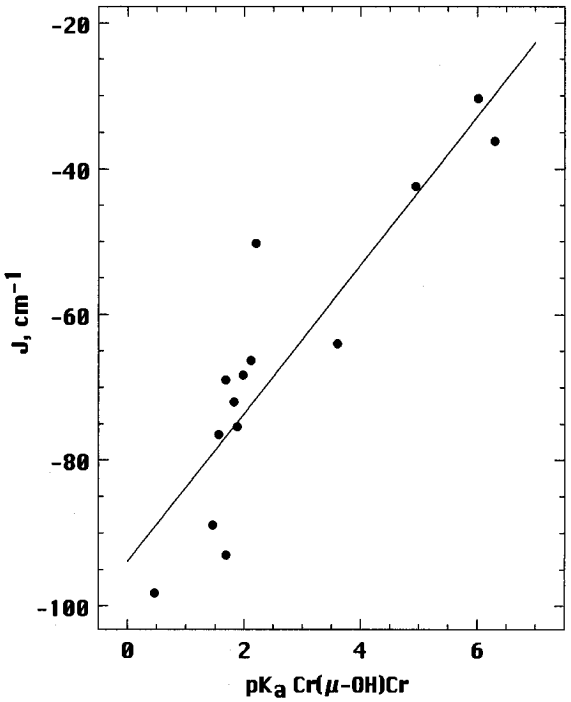

Figure 2. Correlation between antiferromagnetic coupling constants and oxo-bridge basicity for $[(tmpa)Cr(\mu\text{-}O)(\mu\text{-}X)Cr(tmpa)]^{n+}$ dimers, including $X = HS^-$, CO_3^{2-}, $PhPO_4^{2-}$, SO_4^{2-}, and RCO_2^- (R = H, CH_3, CH_2Cl, $CHCl_2$, Ph, Ph-4-CH_3, Ph-4-CF_3, Ph-4-OCH_3, Ph-4-F, Ph-4-Cl). Data for RCO_2^- complexes was taken from refs 11 and 12.

second order perturbation theory, relationship 1 was proposed[2]

$$J = K - 2b^2(1/U + 1/\Delta) \approx -b^2/9U$$

$$b = E(e_u^*) - E(Cr,3d,t_{2g}) \approx 2V^2/\Delta \qquad (1)$$

$$\Delta = E(Cr,3d,t_{2g}) - E(O^{2-},2p)$$

to account for J in quantum mechanical terms. In this equation, K is the direct ferromagnetic exchange integral involving only the metal 3d atomic orbitals, U is the 3d Coulomb energy, Δ represents the energy difference between Cr(III) 3d t_{2g} and O^{2-} 2p orbitals in the isolated ions, and V stands for the 3d−2p hybridization matrix element, which is proportional to the Cr(3d)−O(2p) bonding overlap.

On this basis, J should be primarily responsive to the bonding parameter V, since K is negligibly small for Cr···Cr separations larger than 3 Å.[16] Furthermore, both U and Δ are not expected to vary significantly from one $Cr(\mu\text{-}O)(X)Cr$ system to another, provided that fluctuations in ligand field strength among the various X groups are small and π-bonding interactions between Cr(III) t_{2g} and tmpa pyridyl π^* orbitals are essentially constant throughout the series. Thus, to the extent that $pK_a(Cr(OH)Cr)$ values are inversely proportional to V,[2] our finding of a consistent correlation between antiferromagnetic coupling constants and oxo bridge basicity agrees with the theoretical prediction. It is clear, however, that a better relationship should pertain between J and the energy difference between e_u^* and $e_g(t_{2g})$ molecular orbitals. Indeed, dynamic correlation and relaxation effects must be coupled with the active electron approximation in order for theoretically-predicted J values to agree reasonably well with actual values.[2] We also note that theoretical calculations with σ-donor model ligands consistently predict that $E(b_{2g}) \approx E(b_{1u}) < E(e_g)$ for linear (D_{4h}) CrOCr dimers,[2,3] while experimental magnetic, spectroscopic and electrochemical findings strongly support the ordering $E(e_g) < E(b_{2g}) < E(b_{1u})$ in the presence of tmpa ligands, whose π-accepting ability must be taken into account.

Acknowledgment. R.A.H. thanks the Welch Foundation (Grant D-735) for support of this research.

Supporting Information Available: Tables giving a structure determination summary, atomic positional coordinates, complete bond lengths and angles, H atom coordinates, and anisotropic displacement coefficients for $[(tmpa)Cr(\mu\text{-}O)(\mu\text{-}CO_3)Cr(tmpa)](ClO_4)_2 \cdot 2H_2O$ (10 pages). Ordering information is given on any current masthead page.

IC951214Y